This file was created by scanning the printed publication. Text errors identified by the software have been corrected: however some errors may remain.

SCION

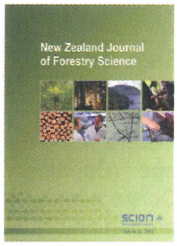

New Zealand Journal of Forestry Science

42 (2012) 1-13

www.scionresearch.com/nzjfs

published on-line: 10/01/2012

Maps and models of density and stiffness within individual Douglas-fir trees

Christine L. Todoroki[1,*], Eini C. Lowell[2], Dennis P. Dykstra[2] and David G. Briggs[3]

[1] *Scion, Private Bag 3020, Rotorua 3046, New Zealand*

[2] *Research Forest Products Technologists, U.S. Forest Service, Portland Forestry Sciences Laboratory, Portland, Oregon, USA*

[3] *Stand Management Cooperative and Precision Forestry Cooperative, University of Washington, Seattle, Washington, USA*

(Received for publication 2 February 2011; accepted in revised form 4 November 2011)

*corresponding author: christine.todoroki@scionresearch.com

Abstract

Spatial maps of density and stiffness patterns within individual trees were developed using two methods: (1) measured wood properties of veneer sheets; and (2) mixed effects models, to test the hypothesis that within-tree patterns could be predicted from easily measurable tree variables (height, taper, breast-height diameter, and acoustic velocity).

Sample trees comprised an assortment of 25 coastal Pacific Northwest Douglas-fir (*Pseudotsuga menziesii* (Mirb.) Franco) trees grown on three sites under a range of thinning regimes. At harvest, trees were 36 years old on one site, and 45 and 51 on the other two. After felling and crosscutting, bolts were peeled into veneer, labelled, dried, weighed, measured, and non-destructively tested using a Metriguard 2600™ veneer tester. The labels allowed each sheet to be tracked back to the peeler bolt and consequently to the position within the parent tree from which it came, and the measurements allowed calculation of veneer density and, after application of the fundamental equation for propagation of sound, veneer stiffness.

Maps of each parent tree created from the veneer data clearly demonstrated regions of higher density and stiffness. Furthermore, within each tree, density was approximately normally distributed, while stiffness tended to have moderate negative skew. Maps developed using mixed effects models showed very good correspondence between measured and predicted patterns, particularly for density. Despite differences in age, site and silviculture, results from this study suggest that it is possible to predict within-tree wood properties using easily measurable tree variables.

Keywords: density; stiffness; Douglas-fir; mixed effects models; REML

Introduction

Wood density and stiffness are known to vary by species, by tree and within individual trees. For Douglas-fir (*Pseudotsuga menziesii* (Mirb.) Franco), one of the densest and stiffest softwood species in North America, density varies radially from pith to bark, i.e. from juvenile wood (often considered to be the first 20 rings from the pith (Fahey et al., 1991)) to mature wood, and vertically from stump to apex (Kennedy & Warren, 1969; Megraw, 1986; Jozsa et al., 1989; Kennedy 1995).

Density variation in the radial direction is non-linear. In the first 15-20 years of growth it is relatively low, thereafter it rapidly increases until about 30 years of age, after which it either increases slightly, or plateaus with subsequent growth (Jozsa & Kellogg, 1986). Similar trends are reported by Megraw (1986), Gaffrey et al. (1999), and Gartner et al. (2002). In the vertical direction and for the same cambial age, density tends to decrease with increasing height. However, in comparison to horizontal trends, vertical density patterns have proved difficult to model (Gaffrey et al., 1999).

© 2012 New Zealand Forest Research Institute Limited, trading as Scion

ISSN 0048-0134 (print)
ISSN 1179-5395 (on-line)

Because wood density influences wood stiffness, or modulus of elasticity (MOE), stiffness also tends to increase in the transition from juvenile wood to mature wood due to its general increase with cambial age (Bendtsen, 1978; Acuna & Murphy, 2006). Consequently, wood from upper logs with a higher proportion of juvenile wood content would be expected to be of lower stiffness. This expectation has been realised in lumber studies by Barrett and Kellogg (1991) and in studies of small clear specimens by Langum et al. (2009). In the latter study, specimens with the highest stiffness were located in the outermost basal tree regions and those with the lowest stiffness at the top of the trees. However, in comparison to radial relationships, vertical relationships appear weaker.

Stiffness is important in products such as laminated veneer lumber (LVL) and structural plywood, so ideally, it would be desirable to measure or assess stiffness properties prior to production. As this cannot be done, much research effort has focussed on assessing the stiffness of the parent log, stem, or standing tree and exploiting parent-child relationships. Good correlations have been found between acoustic velocities (or time-of-flight measurements) of trees and tree sections, and, for lumber, between acoustic velocities and MOE (Briggs et al., 2008). For veneer, Rippy et al. (2000) found good correlation between the acoustic velocities of logs and the average velocity of veneer from those logs.

Acoustic tools have become widely adopted by industry because they enable rapid assessment of lumber and veneer into quality classes (Sharp, 1985). Such segregation is possible due to the strength of the relationship between the speed of propagation of sound and MOE as determined by the fundamental equation (Bucur, 2006):

$$MOE = \rho \times v^2 \quad [1]$$

where ρ is the density of the material (kg m^{-3}) and v is the velocity of sound (m s^{-1}).

In veneer, acoustic velocity is sensitive to knots, holes, and when waves are propagated perpendicular to the grain, are sensitive to lathe damage (Wang et al., 2001). Acoustic velocity is also affected by moisture content. However, Brashaw et al. (1996) found that while velocities in dry Douglas-fir veneer were about 1000 m s^{-1} less than that of green Douglas-fir veneer, the two were highly correlated.

The variation and range of within-tree properties can be visualised using wood property maps. Over the years, wood property maps have advanced from coarse grey scale maps of averaged properties (Evans et al., 1995; for *Pinus radiata* D.Don), to high resolution maps using sequential colour schemes (Mora & Schimleck, 2009; for *Pinus taeda* L.). At the time of preparing this study, no spatial maps, or models, of within-tree density or stiffness for individual trees were found in the literature.

In this study, one of the large information gaps in operational forestry and tree improvement programs (Jayawickrama et al., 2009): understanding within-tree variation is addressed. To aid understanding, spatial colour-coded density and stiffness maps for an assortment of Douglas-fir trees that vary in age, site and silvicultural history were developed. Maps were constructed in a novel way; by reassembling veneer sheets into their original within-tree positions. The spatially allocated veneer data were then used to develop predictive models of within-tree wood density and stiffness, with the aim being to test the hypothesis that density and stiffness patterns can be predicted from easily measurable variables – namely diameter at breast height, tree height, taper, and acoustic velocity.

Method

Veneer Sample

The veneer sheets selected for this analysis were obtained from an assortment of Douglas-fir trees grown under a range of conditions and silvicultural treatments. The trees, derived from a larger study (Briggs et al., 2008), grew in three research installations (Nos. 803, 805 and 808) in the coastal Pacific Northwest of the USA (Table 1). Each installation was established between 1987 and 1989 and comprised four treatment plots, representing possible commercial thinnings, and a control plot with no thinnings. The treatment regimes ranged from repeated thinning operations (at high and low densities) to minimal and delayed thinning operations. Regimes were specified by relative density (RD) a continuous scale, expressed as basal area divided by the square root of quadratic mean stand diameter, representing the level of competition within a stand (Curtis, 1982). The treatment regimes and dates and stand ages when thinning occurred, are summarised in Table 2.

The trees, when felled, were 51 years of age at Installation 803, 36 years at 805, and 45 years at 808. Prior to felling, time of flight (measured in µsec, over a one metre distance centred at breast height, i.e. at 1.4 m above ground) was measured on all trees using TreeSonic™ equipment (Fakopp Bt. Agfalva, Hungary). These measurements were converted into velocity by taking the inverse. After felling, each tree was measured, delimbed, and the merchantable boles crosscut at the harvesting site into long logs with target lengths of 10.7 m. At the mill, the long logs were crosscut into mill-length logs (5.3 m). Each of these mill-length logs was crosscut into two veneer bolts, each 2.6 m long. Bolts were steamed, peeled, and the veneer dried. During the peeling process, a tracking methodology was used that allowed each sheet to be

© 2012 New Zealand Forest Research Institute Limited, trading as Scion
ISSN 0048-0134 (print)
ISSN 1179-5395 (on-line)

TABLE 1: Description of installations in the Pacific Northwest of North America.

Installation	803	805	808
County & State	Mason, WA	Skagit, WA	Polk, OR
Date planted (month, year)	January 1955	January 1970	December 1960
Installation establishment year	1987	1988	1989
Date Harvested (month, year)	November 2005	November 2005	October 2005
Age at harvest (years)	51	36	45
SI (m)	44	49	40
QMD (cm)	36	30	33
HT40 (m)	38	32	31
Latitude	N 47°16'49.41"	N 48°19'7.55"	N 44°57'1.26"
Longitude	W 123°26'6.64"	W 122°8'49.26"	W 123°40'44.41"
Elevation (m)	175	168	762
Slope (%)	0	15	5
Aspect (degrees)	0	90	360
Parent Material	Glacial Till	Glacial Till	Unk
Soil Type	Mohrweis gravelly loam/ Astoria clay loam	Tokul	Luckiamute, very shaly loam

SI =site index at 50 years breast-height age (King, 1966);
QMD =quadratic mean DBH;
HT40 = average height of the 40 largest trees by DBH.

traced back to the peeler bolt and consequently to the position within the parent tree from which it came. Each veneer sheet from a particular bolt was labelled with the bolt number and the order in which it was peeled from the bolt. Occasionally equipment malfunctions occurred, so some sheets were removed from the final data set, after reconciling data files.

Full veneer sheets had dry target sizes of 2.6 m in length, 1.3 m in width, and 3.8 mm in thickness. Due to clipping, shrinkage, and peeling mechanisms, actual dimensions of sheets were subject to variation. Therefore, all sheets were measured and weighed and the actual measurements used in the calculation of veneer sheet density, defined as sheet mass divided by the product of length, width, and thickness. Veneer sheets were also photographed and non-destructively tested using a Metriguard 2600™ veneer tester (Metriguard Inc., Pullman, WA, USA). Up to four tests were conducted per sheet, and the mean stress-wave transit time recorded. Readings were taken close to both ends of the veneer sheet and at 1/3 and 2/3 the length of the sheet as indicated in Figure 1. In some cases, knot whorls, grain disturbance, or natural fracture lines, prevented a reading from being obtained with the Metriguard tester. When transit time readings were available, stiffness was calculated according to the wave equation (Equation 1).

TABLE 2: Treatment regime for the Douglas-fir installations from which veneer sheets were obtained.

Treatment	Thinning Regime	Relative Density (RD) Trigger Sequence	Thinning Date(s) for each Installation (Age when thinned)		
			803	805	808
A	Control		x	x	x
B	Minimal	RD55-RD30, no further thinning	1987 (33)	1990 (21)	1991 (31)
C	Delayed	RD65-RD35, no further thinning	none	none	1993 (33)
D	Light	RD55-RD30, subsequent thinnings at RD50-RD30	1987 (33)	1990, 2004 (21, 34)	1993 (33)
E	Heavy	RD55-RD35; RD 55-RD40, subsequent thinnings RD60-RD4	1987 (33)	1996 (27)	1991 (31)

© 2012 New Zealand Forest Research Institute Limited, trading as Scion
ISSN 0048-0134 (print)
ISSN 1179-5395 (on-line)

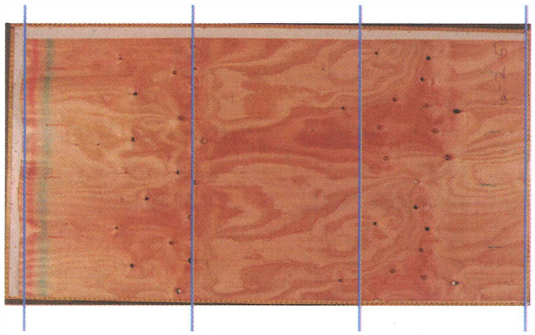

FIGURE 1: Veneer sheet showing approximate positions where stress-wave transit times were recorded.

Wood property maps were constructed for each tree by reassembling the full sheets into the bolts from which they had been peeled, and the bolts into the logs from which they had been cut. Half-sheets peeled from within the heartwood zone, although not analysed, were reassembled to obtain the correct spatial location within the tree relative to the core.

To develop robust models, those trees that demonstrated the greatest number of contiguous veneer sheets, whilst also spanning the range of silvicultural treatments and the three installations were selected for further analysis. In all, 1360 veneer sheets from 20 trees were analysed and used in the development of predictive regression models. All veneer from an additional set of five trees was set aside for model validation. The 20 trees used in the model development phase ranged in diameter at breast height (DBH) from 30.2 to 48.5 cm, in height (H) from 28.2 to 40.9 m, and in taper (T, calculated as the ratio of stump diameter, to tree height less stump height) from 1.0 to 1.8 cm m^{-1}. Standing tree acoustic velocities (V) ranged from 3.1 to 4.4 km s^{-1} (Table 3). Of the validation set, one tree was slightly smaller (Tree 22 with DBH at 28.7 cm and H at 27.3 m), while another tree had a lower acoustic velocity (Tree 23, 2.9 km s^{-1}).

Colour-coded wood property maps

Colour maps of wood properties were developed using the software R (R Development Core Team, 2008) by allocating each veneer sheet to its correct spatial position within the parent tree using the methodology described above. Veneer sheets were coloured using a sequential colour scheme according to the density or stiffness value. Missing sheets were assigned white, and in cases for which stiffness data were absent, sheets were coloured black.

Transformation of veneer indices to metric equivalents

The actual radial distance of the veneer sheet from the pith was determined through a nonlinear transformation of the veneer index, i. The radial distance, *r*, was calculated assuming that the peeled veneer followed the general form given by Archimedes spiral, and had a constant core size, assumed here to be 8.9 cm, for each bolt (Equation 2). A factor of 5% was included to allow for radial shrinkage, *s,* (Simpson & TenWolde, 1999). A linear transformation was applied to the vertical veneer index, *j*, to obtain the actual distance of the veneer sheet from the base of the tree. Bolt height, *h*, was calculated at the mid-point of each bolt, and stump height added to the calculation (Equation 3).

$$r = \sqrt{\frac{iwt}{\pi(1 - s)} + \left(\frac{core}{2}\right)^2} \qquad [2]$$

$$h = bolt \times j - \tfrac{1}{2} \times bolt + stump \qquad [3]$$

Where: *w* is the sheet width (cm)
t, the sheet thickness (cm)
s, the radial shrinkage factor (as a decimal)
core, the diameter of the core (cm)
i is the radial veneer index, i.e. the sheet count from the core
j is the vertical veneer index, based on the parent bolt number and counted from the base of the stem
bolt, the length of bolt (m) and
stump, the height of the stump (m), obtained when each tree was felled.

Mixed effects regression models

The response variables in the mixed effects models, veneer density or stiffness, were first analysed in plots to determine if the underlying data frequency distribution was normally distributed. Departures from normality were tested using the Shapiro-Wilk test of normality (Shapiro & Wilk, 1965) and the D'Agostino skewness test (D'Agostino, 1970) with interpretation of the skewness number, *sk*, following the rule of thumb suggested by Bulmer (1979):

- If $sk < -1$ or $sk > +1$, the distribution is highly skewed.
- If $-1 < sk < -0.5$ or $+0.5 < sk < +1$, the distribution is moderately skewed.
- If $0.5 < sk < +0.5$, the distribution is approximately symmetric.

Predictor variables included combinations of spatial variables (veneer indices or metric equivalents) and tree variables (H, D, T, V and V^2). Interactions between predictor variables were also included in the models. Plots of predictor variables were analysed, and in cases where curvilinear relationships were apparent, non-linear transformations were evaluated.

© 2012 New Zealand Forest Research Institute Limited, trading as Scion

ISSN 0048-0134 (print)
ISSN 1179-5395 (on-line)

TABLE 3: Sample statistics of 25 Douglas-fir trees: 20 used in model development, and a further five trees augmenting model validation. For treatment details see Table 2.

Tree	Installation	Treatment	DBH (cm)	Height (m)	Taper (cm m^{-1})	Acoustic velocity (km s^{-1})
Trees used in model development						
1	803	A	37.1	35.7	1.2	4.2
2	803	B	48.3	40.0	1.3	3.6
3	803	C	39.4	39.7	1.1	3.9
4	803	C	43.4	39.5	1.3	4.1
5	803	D	40.6	37.9	1.2	4.4
6	803	D	43.4	37.5	1.3	4.1
7	803	D	45.7	40.9	1.3	3.9
8	803	E	30.2	34.2	1.0	3.9
9	803	E	33.5	32.1	1.1	4.1
10	803	E	36.1	34.5	1.1	3.7
11	805	A	35.8	33.0	1.3	3.1
12	805	B	40.9	31.4	1.5	3.9
13	805	C	34.5	33.2	1.3	3.1
14	805	D	46.5	32.4	1.5	3.3
15	805	E	37.1	32.4	1.3	3.7
16	808	A	34.0	28.2	1.3	4.0
17	808	B	48.5	31.3	1.8	3.7
18	808	D	45.0	29.1	1.6	3.9
19	808	E	39.1	30.9	1.3	4.0
20	808	E	45.2	31.4	1.4	3.6
Trees used to augment model validation						
21	803	C	34.0	36.3	1.1	4.0
22	803	D	28.7	27.3	1.1	3.9
23	805	A	31.0	31.3	1.2	2.9
24	808	A	41.1	31.1	1.4	4.1
25	808	B	47.8	32.3	1.6	4.0

Linear mixed-effects models were fitted using the Restricted Maximum Likelihood (REML) method. This method was used, rather than using site averages and ordinary regression models, because sampling was not random on sites. Modelling was performed using the software R with the lme function. Conditional *t*-tests and *F*-tests (Pinheiro & Bates, 2000) were applied to test the significance of individual variables using a significance level of 0.05. When more than one variable was found to be significant, the value of adding the extra variable to the model was considered by comparing the Akaike information criterion (AIC, Akaike, 1974), the root mean square error (RMSE), and the mean absolute percentage error (MAPE) of the predictions from the resulting equations (as in Fehrmann et al., 2008).

Fit statistics were supplemented by normal probability plots of residuals. Diagnostics also included colour plots of the fitted wood property values, normal probability plots, and plots of residuals versus fitted values for both model and validation sets of data.

Results

Within-tree veneer wood property distributions

Veneer density within individual trees was approximately normally distributed (Figure 2). All trees, except for Tree 17 which had moderate skew (*sk* = 0.53), were approximately symmetric in distribution. By the Shapiro-Wilk test, 14 of the 20 trees were well approximated by the normal distribution. However the *p*-value for Tree 17 and five other trees (2, 4, 9, 13, 20) fell below the significance threshold suggesting that veneer density data for these tree did not come from normal distributions.

Distributions of veneer stiffness tended to be moderately negatively skewed (i.e. left tailed) for the majority of trees. Data from five trees (11, 13, 14, 15, 18) were well approximated by the normal distribution, but *p*-values for the remainder of trees were below the significance threshold.

© 2012 New Zealand Forest Research Institute Limited, trading as Scion

ISSN 0048-0134 (print)
ISSN 1179-5395 (on-line)

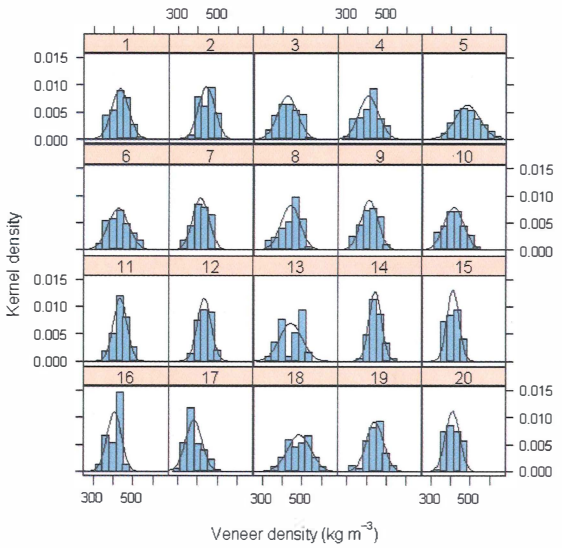

FIGURE 2: Within-tree veneer density distributions.

The sample of 20 Douglas-fir trees used in model development had an average of 66 full veneer sheets per tree. This varied from a minimum of 22 sheets for one tree (Tree 16) to a maximum of 108 sheets for another (Tree 4). The validation data set, with more missing sheets and fewer contiguous sheets than the model dataset, comprised an average of 32 sheets per tree. Veneer sheet counts and summary wood property statistics (mean and standard deviation) of the veneer sheets for each tree are provided in Table 4.

The coefficient of variation (s.d. divided by the mean) averaged 0.10 for density and 0.28 for stiffness. The greater variation associated with stiffness was attributed to the additional factor included in the calculation of stiffness; i.e. stress wave transit time which in turn had a coefficient of variation of 0.16. For those sheets with four transit times recorded, individual measurements deviated from the mean of these measurements by 5% on average. Nearly three-quarters of veneer sheets tested four times had transit times that deviated from the mean by less than 10%, and 95% had transit times within 20% of the mean value. However in three of the 1360 veneer sheets, deviation from the mean exceeded 50%.

Colour-coded wood property maps: measured data

There was considerable variation in wood properties within individual trees. For about 95% of the sample, veneer density ranged from 322 to 535 kg m^{-3} and veneer stiffness from 4.0 to 17.9 GPa. The lowest veneer density of 292 kg m^{-3} was recorded for Tree 17 near the core in the lower section of the tree (at the second sheet from the core and the second bolt from the base). Tree 17, grown under a minimal thinning regime, was the least dense tree on average (380 kg m^{-3}). Two other trees (Trees 4 & 16), grown on plots with no thinning, also recorded relatively low average densities (408 and 406 kg m^{-3} respectively). However, low mean density was also recorded for two trees grown under repeated thinning regimes (Trees 10 & 20, 414 and 409 kg m^{-3} respectively).

TABLE 4: Sample statistics of the veneer sheets peeled from 25 Douglas-fir trees.

Tree	No. of sheets	Density (kg m^{-3})		MOE (GPa)	
		Mean	s.d.	Mean	s.d.
1	66	433	43	11.3	3.4
2	106	441	42	11.0	3.1
3	82	425	50	11.5	3.4
4	108	408	50	10.5	3.8
5	98	483	63	14.0	4.1
6	97	426	52	10.8	3.4
7	104	413	41	10.7	3.0
8	51	440	49	12.8	2.8
9	57	412	44	10.2	3.5
10	54	414	51	11.6	3.4
11	47	435	35	9.5	2.8
12	59	432	35	9.9	3.1
13	34	443	57	11.6	2.9
14	54	443	32	8.8	2.2
15	28	411	31	10.5	2.4
16	22	406	36	10.7	2.7
17	104	380	42	8.9	2.8
18	66	486	59	11.9	2.4
19	51	442	44	11.6	3.7
20	72	409	36	9.7	2.8
21	32	430	47	12.0	2.4
22	18	420	41	10.6	3.3
23	10	445	33	10.2	3.5
24	58	435	34	11.3	3.3
25	47	449	51	11.3	3.5

The veneer sheet of maximum density was peeled from a tree grown under a repeated thinning regime. This tree (Tree 5) exhibited higher than average density (483 kg m^{-3}). Another tree, also grown under repeated thinning, Tree 18, recorded the greatest average density (486 kg m^{-3}). The higher density veneer within these two trees and the lower density within Tree 17 in particular, is clearly evident in the colour maps of Figure 3.

Both high density trees (5 & 18) were amongst the stiffest trees (Table 4, Figure 4). In general, those trees with high average density were also of high average stiffness (cf Figures 3 & 4).

Within all trees, veneer density and stiffness showed a strong tendency to increase in the radial direction.

© 2012 New Zealand Forest Research Institute Limited, trading as Scion

ISSN 0048-0134 (print)
ISSN 1179-5395 (on-line)

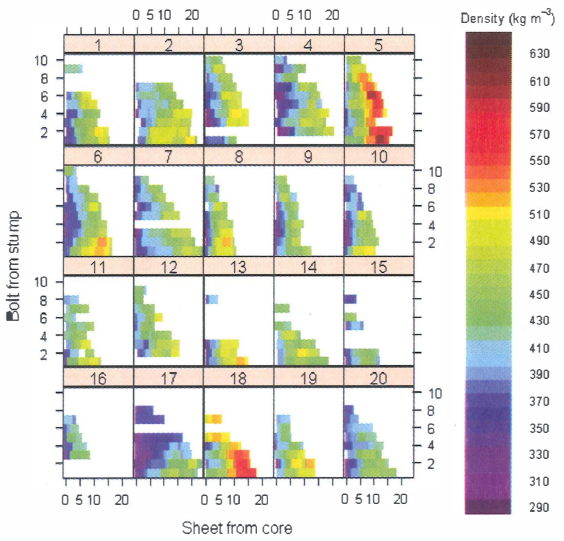

FIGURE 3: Measured density maps within 20 Douglas-fir trees, reassembled from dried veneer sheet data. Blank spaces within profiles indicate that no veneer data was available.

The least dense/least stiff veneer tended to be closer to the tree centre, while the densest was closer to the bark and at the base of the tree. The majority of high-stiffness veneer was located in the outermost tree layers and tended to be in the lower half of the tree.

Density, in a plot against sheet number from core, demonstrated a curvilinear relationship with increasing distance from core (Figure 5). A similar trend was also found for stiffness, particularly for those trees for which

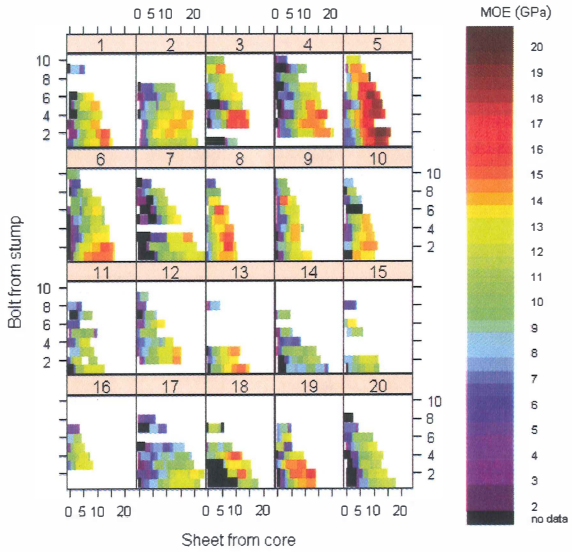

FIGURE 4: Measured stiffness maps within 20 Douglas-fir trees. Black squares indicate sheets with no recorded transit times; blank spaces indicate missing veneer sheets.

data was approximately normally distributed, thus nonlinear relationships were investigated. A quadratic relationship provided a better fit to the density data (R^2 = 0.34), than did a linear relationship (R^2 = 0.28). Square-root (R^2 = 0.31), and logarithmic relationships with transformations of: (a) predictor; and (b) both response and predictor variables (R^2 = 0.32 in each case), also suggested an improved fit. However, the models incorporating logarithmic and square-root transformations were no better, in terms of AIC, RMSE, and MAPE, over the simpler models, hence only the simpler linear models are discussed further.

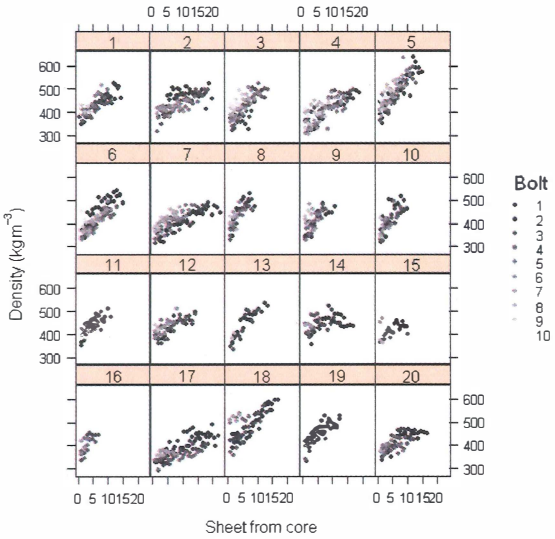

FIGURE 5: Density of veneer sheets plotted against sheet index from core. Veneer from the two lowermost bolts are shown in black, increasingly higher bolts are shown in progressively lighter shades of grey.

Density models

All predictor variables were significant in the best seven models used for estimating density (Table 5). In the simplest additive model containing all five variables, Model D1, AIC was 13858, RMSE 39.2, and MAPE 7.1. Addition of i^2 to Model D2 to account for the nonlinear relationship noted above between radial veneer index and density reduced all three fit statistics: AIC by 95, RMSE by 1.4 and MAPE by 0.2. Further reductions in fit statistics were obtained when interactions were added to the models. A large improvement in fit statistics was obtained when V^2 was included (Models D6 and D7). The best model, in terms of fit statistics, was model D7 with AIC equal to 13164, a RMSE of 30.4, and a MAPE of 5.7. When the veneer indices were replaced with their metric equivalents by substitution into Equations 2 and 3, similar results were obtained. Random effects due to site were greatest for Installation 805 (for

© 2012 New Zealand Forest Research Institute Limited, trading as Scion

ISSN 0048-0134 (print)
ISSN 1179-5395 (on-line)

TABLE 5: Models for predicting within-tree density.

Model	Model form[1]	Development dataset		
		Akaike information criterion (AIC)	Root mean square error (RMSE)	Mean absolute percent error (MAPE)
D1	i+j+D+H+T+V	13858	39.2	7.1
D2	i+j+i^2+D+H+T+V	13763	37.8	6.9
D3	i*j +i^2+D+H+T+V	13719	37.1	6.8
D4	i*j +i^2+D+H*T+V	13579	35.3	6.5
D5	i*j +i^2+H*T+(D+T)*V	13479	34.1	6.4
D6	i*j +i^2+H*T+(D+T)*V+i*V^2	13196	30.7	5.8
D7	i*j +i^2+H*T+(D+T)*V+(D+i)*V^2	13164	30.4	5.7

[1] Variables:
i = radial veneer index; j = vertical veneer index;
V = acoustic tree velocity (km s^{-1}) D = tree diameter at breast height (cm);
H = tree height (m); T = taper (cm m^{-1})

which the intercept was raised by 11.55 kg m^{-3} with Model D7) and least for Installation 808 (-12.89 kg m^{-3}). Installation 803 lay between those two extremes (1.34 kg m^{-3}). Model estimates and statistics for the fixed effects of Model D7 are given in Table 6.

Predicted individual tree density maps

The improvement in model predictability can be visualised using the colour concept developed above for the measured veneer sheet density data. Figure 6 shows estimated density after application of models D1, D3, D5, and D7 to the first five trees in the sample. The relatively poor performance of Model D1 is readily apparent when contrasted with the data assembled from actual measurements (refer top row Figure 3). Improvements in colour matches are increasingly evident in the progression through models D3, D5, and finally D7 which embodies a better representation of density data near the core and in the outer layers.

TABLE 6: Parameters and statistics for Model D7 for predicting density within individual Douglas-fir trees.

Variable[1]	Value	Std. Error	*p*-value
Intercept	-4090.75	1369.90	0.0029
i	7.60	1.67	0.0000
j	7.82	0.70	0.0000
i^2	-0.53	0.04	0.0000
H	36.56	3.04	0.0000
T	-1602.9	179.4	0.0000
D	249.02	37.80	0.0000
V	2390.35	751.88	0.0015
V^2	-398.35	103.31	0.0001
i:j	-1.05	0.11	0.0000
H:T	-35.76	2.46	0.0000
D:V	-123.08	20.36	0.0000
T:V	681.82	43.80	0.0000
i:V^2	0.88	0.09	0.0000
D:V^2	15.35	2.71	0.0000

[1] Variables as defined in Table 5

Stiffness models

All the models tested for predicting stiffness were less satisfactory in terms of fit statistics than those for density. The best three models are given in Table 7. The addition of each independent variable provided small improvements to the model in most cases. However, unlike the predictive models for density, models with interactions showed only a slight improvement over the

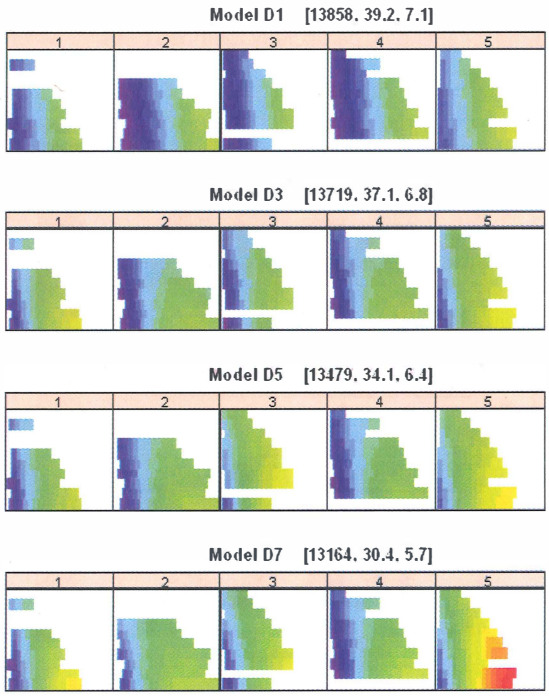

FIGURE 6: Visualisation of model performance (with fit statistics [AIC, RMSE, MAPE]) in predicting within-tree density for a sample of trees (Trees 1 to 5).

© 2012 New Zealand Forest Research Institute Limited, trading as Scion

ISSN 0048-0134 (print)
ISSN 1179-5395 (on-line)

TABLE 7: Models for predicting within-tree veneer stiffness

Model	Model Form[1]	AIC	RMSE	MAPE
S1	$i+j+i^2+H+T+D+V+V^2$	5385	2.26	20.6
S2	$i+j+i^2+H*T+(D+T)*V+V^2$	5317	2.19	20.1
S3	$i+j+i^2+H*T+(D+T)*V+i*V^2$	5287	2.15	19.9

[1] Variables as defined in Table 5

simpler additive models. Interactions between H and T were highly significant, as were interactions between D and V, and T and V (Models S2 and S3). Interactions and predictor variables were also significant in the equivalent models that replaced the veneer indices with metric equivalents using Equations 2 and 3. Furthermore, fit statistics for the metric equivalents followed the same trend with improved model statistics resulting following the addition of interactions to the models. For Model S3, random effects due to site were, like density, greatest for Installation 805 (for which the intercept was raised by 0.18 GPa). However random effects were least for Installation 803 (-0.15 Pa) and Installation 808 had the intermediary value of -0.03 GPa. Coefficients and standard errors of model S3 are given in Table 8.

Validation

Application of model D7 to predict density within the 20-tree dataset showed good correspondence between actual (Figure 3) and predicted within-tree density for each tree (Figure 7). Application of model S3 to predict stiffness within the 20-tree dataset also showed a reasonable level of correspondence between actual (Figure 4) and predicted (Figure 8) results, but the correspondence between actual and predicted stiffness was not as good as that between actual and predicted density. The normal probability plot of the standardised residuals (top row of Figure 9) was better for density than stiffness, and plots of standardised residuals fluctuated around zero for both the model development dataset (middle row of Figure 9) and the model validation dataset (bottom row of Figure 9), though there appeared to be some bias associated with individual validation trees, particularly Tree 24. There were also some observations that produced residuals larger than the majority of others residuals for both density and stiffness values.

TABLE 8: Parameters and statistics for Models S3 for predicting stiffness within individual Douglas-fir trees.

Variable[1]	Value	Std. Error	p-value
Intercept	115.72	18.42	0.0000
i	0.42	0.12	0.0005
j	0.08	0.03	0.0109
i^2	-0.03	0.00	0.0000
H	1.42	0.24	0.0000
T	-43.03	12.52	0.0006
D	1.32	0.33	0.0001
V	-64.05	7.21	0.0000
V^2	6.79	0.82	0.0000
H:T	-1.35	0.19	0.0000
D:V	-0.35	0.09	0.0002
T:V	20.75	3.02	0.0000
$i:V^2$	0.05	0.01	0.0000

[1] Variables as defined in Table 5

Discussion

All Douglas-firtrees analysed in this study demonstrated considerable variation in density and stiffness in radial and vertical directions. Radial differences were more pronounced than vertical differences. This can be seen both through observation of the wood property colour maps (Figures 3 & 4) and through the model statistics (Tables 6 & 8) relating to the radial and vertical veneer indices. Maps of within-tree density and stiffness, both measured (from veneer sheets) and predicted (through mixed effects models), demonstrated that veneer of higher density and higher stiffness was located in the outermost layers of the tree, particularly near the base, as also noted by Rippy et al. (2000) and Langum et al. (2009). Because trees of a certain age have a higher proportion of mature wood at the base than higher up, it therefore follows that a greater proportion of high density and high-stiffness veneer will be located in the lower tree sections.

The veneer sheets were peeled from bolts until a core diameter of approximately 8.9 cm was attained. This core diameter was assumed to be constant, however, in reality, the core size was not fixed, and some bolts had larger cores than others. No data were available within the core zone, thus the models presented here are valid only for that range extending beyond the core. This has implications on mean tree properties. As calculated here, mean tree properties excluded the region (assumed to be 4.45 cm) from pith to core containing low-density low-stiffness wood. Due to taper and ovality, outer regions of high-density high-stiffness wood were also excluded. Thus, in the absence of taper and ovality, mean tree veneer density/stiffness would be expected to exceed mean whole-tree density, and in the presence of taper and ovality, we would expect some compensatory effects.

© 2012 New Zealand Forest Research Institute Limited, trading as Scion

ISSN 0048-0134 (print)
ISSN 1179-5395 (on-line)

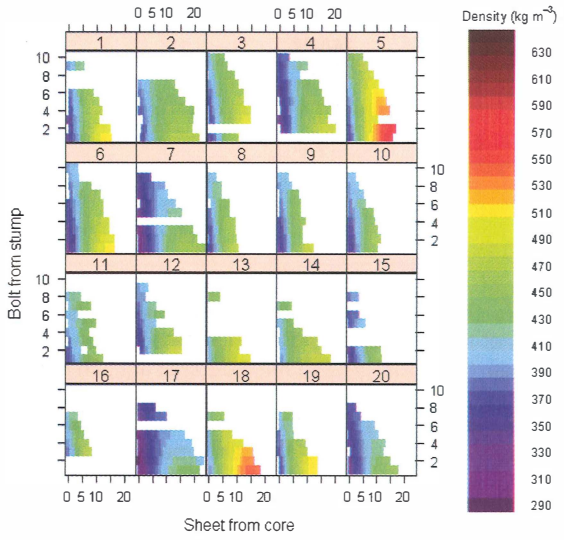

FIGURE 7: Predicted density maps of 20 Douglas-fir trees using Model D7.

In addition to variation in core size, and hence radial measures, there was also variation associated with density, stress wave transit times, and hence stiffness measures. Variation within density components (veneer length, width, thickness, weight) was relatively small. Variation within transit times was larger with the difference between successive measurements on the same sheet being about 5% on average, however larger deviations were noted for some veneers sheets. For example, the sheet shown in Figure 1 was one of the three cases noted above where a transit time reading deviated from the mean of the four readings by more 50%. The outlier may have been caused by the holes in the sheet (near the second vertical line from the left). This contrasts to the other clear veneer regions, without knots or holes, where the other readings were recorded. In addition to knots and holes, differences between successive measurements on the same sheet could be due to rips, lathe damage, and other grain irregularities. One method that could be applied to reduce irregularities in successive transit times would be to calculate the median, rather than the mean. In this way sheets with one or two readings would be unaffected. For those with 3 or 4 readings, the lowest and highest values would be effectively discarded. An alternative approach, but possibly less practical, would be to take a larger sample of measurements on each veneer sheet.

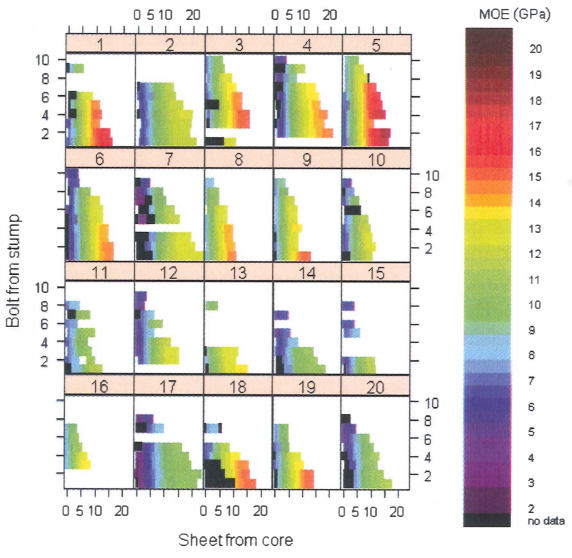

FIGURE 8: Predicted stiffness maps of 20 Douglas-fir trees using Model S3.

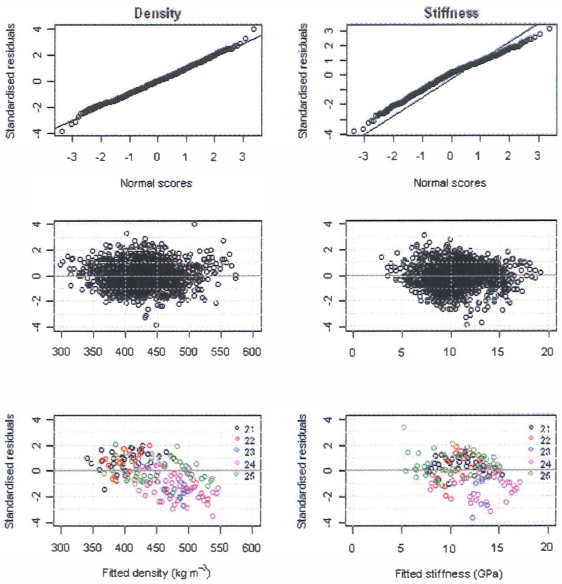

FIGURE 9: Normal probability plots and standardised residuals calculated from the D7 density and S3 stiffness models. Model datasets (Trees 1 to 20) are shown in rows 1 and 2, and validation dataset (Trees 21 to 25) in row 3.

Using visual inspection of the colour plots, predictions of density and stiffness (through application of models D7 and S3 respectively) appeared to be reasonably close to the actual measurements. Through visualisation it was also clear that density models incorporating more interactions provided closer fits to the measured data with the simple additive model (D1, Figure 6) demonstrating reduced colour ranges with shades of yellow through red notably absent from density predictions, though present in both measured profiles and profiles generated using Model D7.

Random effects due to site were greatest for Installation 805 which had the greatest site index at

© 2012 New Zealand Forest Research Institute Limited, trading as Scion

ISSN 0048-0134 (print)
ISSN 1179-5395 (on-line)

49 m. Random effects were least for Installation 808 which had the lowest site index at 40 m for the density models, but this was not the case with stiffness for which differences due to site were quite small.

In general, models for predicting density were more satisfactory than those for predicting stiffness. This was shown, not only through model fit statistics (AIC, RMSE, and MAPE), but also through the colour maps and model validation plots. Stiffness models showed deviation from normality in some trees (refer Shapiro-Wilk test results described above, and Figure 9) and were based on datasets comprising more missing data than their density counterparts, which may have compromised model development. Other sources of error may have been introduced through the unbalanced dataset (refer Table 3) and through other factors not included in the models, such as tree age, site factors (elevation, aspect, rainfall, soil), and silvicultural treatments.

Conclusion

Colour maps of within-tree wood properties clearly demonstrated changing density and stiffness patterns within individual Douglas-fir trees. In general, high density trees were also the stiffest.

Density within trees was successfully predicted using models based on easily measurable tree variables, with the best models being those that incorporated interactions between tree acoustic velocity and other predictor variables. Given that the trees came from a range of sites and silvicultural treatments, and were of differing ages, the results presented here (via colour maps, model statistics, and independent validation datasets) suggest that the models (particularly Model D7 after conversion to metric equivalents using Equations 2 and 3) could be useful for estimating within-tree density from simple field measurements.

Stiffness, whilst also predicted relatively well by models using simple tree measurements, should be treated with a little more caution as the assumption of normality was violated by some trees. Thus the stiffness models are less reliable than the density models.

The colour-coded wood property profiles, supported by model statistics, added a new dimension to model analysis and validation. The addition of coloured wood properties allowed visual assessment of the quality of the model in terms of how closely the predicted wood property matched the original measured data from a spatial point of view. We recommend that this approach be adopted in future research.

In the research presented here, an assortment of trees from three sites and grown under a range of thinning regimes were analysed. Those differences due to site and silviculture remain to be investigated and will be the focus of future work.

Acknowledgements

This project was funded through the Sustainable Forestry component of Agenda 2020, a joint effort of the USDA Forest Service Research & Development and the American Forest & Paper Association. Research partners include the Stand Management and Precision Forestry Cooperatives and Rural Technology Initiative Program at the University of Washington College of Forest Resources, USFS Pacific Northwest Research Station, and CHH FibreGen. Funds were provided by the USFS Rocky Mountain Research Station, the University of Washington, College of Forest Resources, the USFS Pacific Northwest Research Station, and the USFS Forest Products Laboratory. Collaboration has been further supported through a Joint Venture Agreement between the USDA FS and the New Zealand Forest Research Institute Limited, trading as Scion, and through Future Forests Research Limited, a research partnership between Scion and New Zealand forest industries, funded via FRST contract Diverse Forests CO4X0805.

References

Acuna, M. A., & Murphy, G. E. (2006). Geospatial and within-tree variation of wood density and spiral grain in Douglas-fir. *Forest Products Journal 56*(4), 81-85.

Akaike, H. (1974). A new look at the statistical model identification. *IEEE Transactions on Automatic Control 19*(6), 716-723. doi: 10.1109/TAC.1974.1100705

Barrett, J. D., & Kellogg, R. M. (1991). Bending strength and stiffness of second-growth Douglas-fir dimension lumber. *Forest Products Journal, 41*(10), 35-43.

Bendtsen, A. B. (1978). Properties of wood from improved and intensively managed trees. *Forest Products Journal, 28*(10), 61-72.

Brashaw, B. K., Ross, R. J., & Pellerin, R. F. (1996). Stress wave nondestructive evaluation of green veneer: Southern yellow pine and Douglas fir. In *Proceedings of SPIE 2944, Nondestructive Evaluation of Materials and Composites, Scottsdale, AZ, USA, 3 December 1996. (pp. 296-306).* http://dx.doi.org/10.1117/12.259070

Briggs, D., Thienel, G., Turnblom, E., Lowell, E., Dykstra, D., Ross, R. J., Wang, X., & Carter, P. (2008). Estimating wood stiffness along the trees to product chain: Tools, relationships and silviculture influences. *The Western Forestry and Conservation Association Wood Quality Workshop: Current Research &*

© 2012 New Zealand Forest Research Institute Limited, trading as Scion

ISSN 0048-0134 (print)
ISSN 1179-5395 (on-line)

Developments in Wood Stiffness & Other Key Properties. Vancouver, WA, May 28, 2008, (pp. 85-102).

Bucur, V. (2006). *Acoustics of wood*. (2nd ed.). Berlin, Germany: Springer-Verlag.

Bulmer, M. G. (1979). *Principles of statistics.* New York, USA: Dover Publications.

Curtis, R. O. (1982). A simple index of stand density for Douglas-fir. *Forest Science, 28,* 92-94.

D'Agostino, R. B. (1970). Transformation to normality of the null distribution of g1. *Biometrika*, *57*(3), 679-681.

Evans, R., Downes, G., Menz, D., & Stringer, S. (1995). Rapid measurement of variation in tracheid transverse dimensions in a radiata pine tree. *Appita Journal, 48*(2), 134-138.

Fahey, T. D., Cahill, J. M., Snellgrove, T. A., & Heath, L. S. (1991). *Lumber and veneer recovery from intensively managed young growth Douglas-fir.* (Research Paper PNW-RP-437). Portland, OR, USA: USDA Forest Service, Pacific Northwest Research Station.

Fehrmann, L., Lehtonen, A., Kleinn, C., & Tomppo, E. (2008). Comparison of linear and mixed-effect regression models and a *k*-nearest neighbour approach for estimation of single-tree biomass. *Canadian Journal of Forest Research, 38*(1), 1-9.

Gaffrey, D., Hapla, F., Saborowski, J., Wagner, B., & Megraw, R. A. (1999). Model approaches for estimating the wood density distribution of Douglas-fir. [Modellansätze zur prognose der rohdichteverteilung bei der Duglasie]. *Drevarsky Vyskum/Wood Research, 44*(3-4), 39-59.

Gartner, B. L., North, E. N., Johnson, G. R., & Singleton, R. (2002). Effects of live crown on vertical patterns of wood density and growth in Douglas-fir. *Canadian Journal of Forest Research, 32*(3), 439-447.

Jayawickrama, K. J. S., Ye, T. Z., Gupta, R., & Cherry, M. L. (2009). *Including wood stiffness in tree improvement of coastal Douglas-fir in the US Pacific Northwest: A literature review and synthesis.* Covallis, OR, USA: Forestry Communications Group, Oregon State University.

Jozsa, L. A., & Kellogg, R. M. (1986). *An exploratory study of the density and annual ring width trends in fast-growth coniferous wood in British Columbia.* (CFS Contract Rept. No. 02-80-55-017). Vancouver, BC, Canada: Forintek Canada Corporation.

Jozsa, L. A., Richards, J., & Johnson, S. G. (1989). Relative density. In R. M. Kellogg, (Ed.), *Second growth Douglas-fir: its management and conversion for value: a report of the Douglas-fir task force* (pp. 5-22). Vancouver, BC, Canada: Forintek Canada Corporation.

Kennedy, R. W. (1995). Coniferous wood quality in the future: concerns and strategies. *Wood Science and Technology, 29*(5), 321-338.

Kennedy, R. W., & Warren, W. G. (1969). *Within-tree variation in physical and chemical properties of Douglas-fir.* (FAO Second World Consultation on Forest Tree Breeding. FO-FTB-69-4/4).

King, J. E. (1966). *Site index curves for Douglas-fir in the Pacific Northwest.* (Weyerhaeuser Forestry Paper No. 8). Centralia, WA, USA: Forest Research Center.

Langum, C. E., Yadama, V., & Lowell, E. C. (2009). Physical and mechanical properties of young-growth Douglas-fir and western hemlock from western Washington. *Forest Products Journal, 59*(11-12), 37-47.

Megraw, R. A. (1986). Douglas-fir wood properties. In C. D. Oliver, D. P. Hanley, & J. A. Johnson (Eds.), *Douglas-fir: stand management for the future* (pp. 81-96). (Institute of Forest Resources Contribution No. 55). Seattle, WA, USA: University of Washington, College of Forest Resources.

Mora, C. R., & Schimleck, L. R. (2009). Determination of within-tree variation of *Pinus taeda* wood properties by near infrared spectroscopy. Part 2: Whole-tree wood property maps. *Appita Journal, 62*(3), 232-238.

Pinheiro, J. C., & Bates, D. M. (2000). *Mixed-effects models in S and S-PLUS.* New York, USA: Springer-Verlag.

R Development Core Team. (2008). *R: A language and environment for statistical computing.* Vienna, Austria: R Foundation for Statistical Computing.

Rippy, R. C., Wagner, F. G., Gorman, T. M., Layton, H. D., & Bodenheimer, T. (2000). Stress-wave analysis of Douglas-fir logs for veneer properties. *Forest Products Journal, 50*(4), 49-52.

© 2012 New Zealand Forest Research Institute Limited, trading as Scion

ISSN 0048-0134 (print)
ISSN 1179-5395 (on-line)

Shapiro, S. S, & Wilk, M. B. (1965). An analysis of variance test for normality (complete samples). *Biometrika, 52*(3-4), 591-611. doi:10.1093/biomet/52.3-4.591

Sharp, D. J. (1985). Nondestructive testing techniques for manufacturing LVL and predicting performance. In *Proceedings of the 5th Nondestructive Testing of Wood Symposium* (pp. 99-108). Pullman, WA, USA: Washington State University.

Simpson, W., & TenWold, A. (1999). Physical properties and moisture relations of wood. In *Forest Products Laboratory. 1999. Wood handbook—Wood as an engineering material.* (General Technical Report FPL–GTR–113). Madison, WI, USA: US Department of Agriculture, Forest Service, Forest Products Laboratory.

Wang, J., Biernacki, J. M., & Lam, F. (2001). Nondestructive evaluation of veneer quality using acoustic wave measurements. *Wood Science and Technology, 34*(6), 505-516.

© 2012 New Zealand Forest Research Institute Limited, trading as Scion

ISSN 0048-0134 (print)
ISSN 1179-5395 (on-line)